Catal Lett (2007) 117:25–33
DOI 10.1007/s10562-007-9185-7

Radius of Curvature Effect on the Selective Oxidation of Cyclohexene Over Highly Ordered V-MCM-41

Qinghu Tang · Chuan Wang · Shuangquan Hu · Hui Sun · Yuan Chen · Gary L. Haller · Yanhui Yang

Received: 9 May 2007 / Accepted: 22 June 2007 / Published online: 17 July 2007

Abstract V-MCM-41 mesoporous molecular sieves with similar vanadium content (~0.6 wt.%) and surface area (~700 m^2/g) but different pore sizes (from 1.8 to 2.9 nm) were synthesized. A pore wall radius of curvature effect on the initial rate of catalytic reaction existed when the cyclohexene epoxidation was used as a probe reaction, the larger the pore size, the higher the initial reaction rate. However, the turnover frequencies over a long period (72 h) were constant respect to different pore diameters, which was probably due to the strong pore diffusion limitation in the liquid environment.

Keywords V-MCM-41 · Oxidation of cyclohexene · Radius of curvature effect · Pore diffusion limitation

1 Introduction

Improving the activity and the selectivity of molecular sieve materials is one of the main areas of heterogeneous catalysis research. The incorporation of certain transition metal ions into the zeolite lattices will create catalysts with remarkably enhanced catalytic activities for the partial oxidation of hydrocarbons [1–6]. However, these zeolite materials are restricted to structures having pore diameters less than 1.3 nm [7–10]. Therefore, finding an efficient catalyst for handling bulky organic compound under mild conditions remains a difficult challenge for chemical engineering and biological sciences.

Since the discovery of the M41S family of mesoporous molecular sieves, prepared using a cylindrical micellar surfactant as the template, considerable attention has been paid to the research of these materials [11, 12]. As the best studied member of this M41S group, MCM-41 has attracted more awareness because of its high thermal and hydrothermal stability, narrow pore size distribution with size controllable pores, and uniform shape of the pores over micrometer length scales. These properties make MCM-41 potentially applicable to the separation of proteins and selective adsorption of large molecules from effluents [13–19].

With prospective catalytic applications in mind, the ability to isomorphously substitute Si by a broad range of first-row transition metals has been widely studied [20–27]. Vanadium-containing MCM-41 has received more attention since many oxidation catalysts have vanadium as an active component [25, 28–36]. Epoxidation of cyclohexene over vanadium catalysts is one of the well-studied reactions [37, 38]. Although the mesoporous materials are known as hydrophilic, they are still active in the epoxidation reactions using dry *t*-butyl hydroperoxide (TBHP) as oxidant by adopting modifications to both the catalyst and the reaction conditions [39].

The aim of this work is to test the hypothesis that the activity might be systematically varied by changing the radius of curvature of the pore wall on which the catalytic site is located. Such effect has been discussed recently on gas phase reaction over V-MCM-41 [32, 34, 36]. In order to overcome the doubts that many structural parameters may have a greater effect on the catalytic activity and selectivity than the curvature of pore walls, a series of V-MCM-41 samples were prepared with very long-range ordered structure, different pore sizes, and constant composition by

Q. Tang · S. Hu · H. Sun · Y. Chen · Y. Yang (✉)
School of Chemical and Biomedical Engineering, Nanyang Technological University, Singapore 637459, Singapore
e-mail: yhyang@ntu.edu.sg

C. Wang · G. L. Haller
Department of Chemical Engineering, Yale University, New Haven, CT 06520, USA

applying a recently developed quantitative model [21]. In this contribution, V-MCM-41 samples with similar surface area and vanadium content but different pore diameters will be prepared, the effect of vanadium loading, surfactant chain length and type and pH on the synthesis will be discussed. Partial oxidation of cyclohexene to epoxide will be used as model reaction to test the curvature effect on selective oxidation in the liquid environment.

2 Experimental Section

2.1 Materials

Sources of silica were HiSil-233 (Pittsburgh Plate Glass (PPG)) and tetramethylammonium silicate (10% silica, SACHEM Inc.). The vanadium source was $VOSO_4 \cdot 3H_2O$ (Sigma-Aldrich Chemical Co.). Quaternary ammonium surfactants, $C_nH_{2n+1}(CH_3)_3NBr$, were used to form the template with n = 12, 14, 16 (Sigma-Aldrich Co.) and with n = 10 (American Tokyo Kasei). The surfactant solutions were prepared by ion-exchanging the 29 wt.% $C_nH_{2n+1}(CH_3)_3NBr$ aqueous solution with equal molar exchange capacity of Amberjet-4400(OH) ion-exchange resin (Sigma Co.) by overnight batch mixing. The anti-foaming agent was Antifoam A (Sigma Co.), which is a silane polymer alkyl terminated by methoxy groups. Acetic acid (Fisher Scientific) was used for pH adjustment of the synthesis solution.

2.2 Synthesis

The preparation process is exemplified with the sample V-MCM-41 (C16). The surfactant solution was first prepared. The powder of cetyltrimethylammonium bromide (CTMA · Br, 20.0 g) was dissolved in deionized water (80.0 g) to make 20.0 wt.% solution. Then Amberjet 4400 OH anion-exchange resin (50 mL at the ration of 1 mmol surfactant/mL resin) was added into the solution to exchange Br^- ions with OH^- ions. The ion-exchange process took overnight under vigorous agitation. The resulting solution was filtered and ready for use. The fumed silica HiSil-233 (2.5 g) was added into tetramethylammonium silicate (TMA) aqueous solution (10.4 g) and stirred vigorously for half hours, 50.7 mL deionized water was added to improve mixing. The vanadium aqueous solution (2 wt.% $VOSO_4 \cdot 3H_2O$) was added and stirring continued for another 30 min. Two drops antifoam agent were dropped, followed by adding the surfactant ($C_{16}H_{33}(CH_3)_3N \cdot OH$ 20 wt.%) solution (28.7 g) slowly and continuously. The pH was adjusted by adding acetic acid. Finally the reactant molar ratios were: 0.29 SiO_2 (from TMA): 0.71 SiO_2 (from Hisil 233): 0.27 Surfactant: 86 water; the pH was 11.5. After additional mixing for about 120 min under ambient conditions, this synthesis solution was poured into a polypropylene bottle and placed in the autoclave at 100 °C for 6 days. After cooling to room temperature, the resulting solid was recovered by filtration, washed with deionized water and dried under ambient conditions. The pre-dried white powder was calcined by heating at a constant rate from room temperature to 540 °C over 20 h under He, holding the sample for 1 h at 540 °C with He and 5 h at 540 °C with air to remove the residual surfactant. Since the preparation process may cause some loss of vanadium and silica in the by-products, vanadium content of each sample was measured by ICP (Galbraith Lab., Inc.).

2.3 Characterization

2.3.1 Nitrogen Physisorption

Nitrogen adsorption–desorption isotherms were measured at 77 K with a static volumetric instrument Autosorb-3b (Quanta Chrome). Prior to measurement, the samples were outgassed at 473 K to a residual pressure below 10^{-4} Torr. A Baratron pressure transducer (0.001–10 Torr) was used for low-pressure measurements. The pore size distribution were calculated from the desorption isotherms using the BJH method [40].

2.3.2 X-ray Diffraction (XRD)

In order to determine if the prepared V-MCM-41 has the characteristic hexagonal pore structure after calcination, X-ray diffraction measurement was carried out using a SCINTAG X-ray diffractometer (Cu $K\alpha$, wavelength λ = 1.542 Å).

Convincing evidences (solid-state NMR, X-ray absorption spectroscopy, photoluminescence, UV–vis, Raman, etc.) from previous studies have shown that the vanadium ions (reducible V^{5+}) in this V-MCM-41 catalytic system are tetrahedrally incorporated into the framework of siliceous MCM-41 [21, 36]. The reducibility of vanadium species has been investigated by temperature programmed reduction technique and oxidation titration reported somewhere else [36].

3 Results and Discussion

3.1 Effect of the Vanadium Loading

Nitrogen physisorption was carried out to confirm the ordered structure of V-MCM-41 materials. If the synthesized sample has regular pores, it will show a step increase in the isotherm due to the capillary condensation at a certain

pore size. Figure 1 shows the isotherms of V-MCM-41 with different initial vanadium contents (under constant pH 11.5). Each isotherm shows a step increase at the relative pressure around 0.3–0.4. This demonstrates that all samples have highly ordered regular pore structures. There is also a step increase at around a relative pressure 0.9–1. This is because of the macropore filling, which is generated by interparticle spacing. The sharp steps become smaller with the increase of vanadium content, it indicates that the loss of the V-MCM-41 structural order occurs because of the vanadium incorporation.

X-ray diffraction is one of the most important techniques for characterizing the structures of crystalline or other ordered materials. It has been widely used in the study of MCM-41 materials. The sharp step in physisorption indicates that the sample has uniform mesopores, but does not imply a two-dimensional hexagonal arrangement, which can be demonstrated by XRD. The XRD diffraction peaks do not result from the crystal structures in the atomic range, but from the ordered channel walls of MCM-41. Figure 2 shows the XRD patterns of V-MCM-41 with different vanadium concentrations. A well ordered two-dimensional hexagonal structure can be illustrated from the XRD diffractions, which gives a sharp (100) plane diffraction peak and the diffraction peaks of higher Miller Index planes, (110), (200) and (210). With the increase of vanadium content, the diffraction peaks become broad, the peak intensities decrease, the (110) peak and (200) peak overlap, which indicates that the incorporation of a large amount of vanadium disturbs the structures of V-MCM-41.

In this study, N_2 physisorption isotherms and X-ray diffraction patterns were used as the index to characterize the V-MCM-41 structures. In the case of N_2 physisorption isotherm, the slope of the capillary condensation step strongly correlates with structural order [14, 41]; In the case of XRD, this will be the ratio of the second order hexagonal diffraction peak (110) to the first order (100) diffraction peak areas [21].

Figure 3 shows that the surfactant alkyl chain length has remarkable effect on the formation of V-MCM-41 structures, the longer the alkyl chain, the better the V-MCM-41 structures, indicated by both the slopes of the capillary condensation steps and the ratios of (110) to (100) diffraction peak areas. The critical micellar concentration (cmc) decreases with the alkyl chain length, the dynamic exchange of surfactants between water and micelles is slowed down for larger micelles due to the higher hydrophobicity of the longer chain. The micelles formed with longer chain surfactants have a longer lifetime, the average residence time of surfactant molecule in the micelles increases exponentially with the chain length. As a consequence, the formation of the micellar templates is easier resulting in a good V-MCM-41 structure.

The structure of V-MCM-41 sample prepared with C10 surfactant template (surfactant molecule with 10 carbon atoms chain, produce MCM-41 structures that are among those with the smallest pores with good long range order) is dramatically disturbed by the incorporation of vanadium species. According to previous study, the tetramethylammonium (TMA) group (comes from the tetramethylammonium silicate) has significant effect on the mesoporous structure [21]. In this study, higher TMA concentration (up

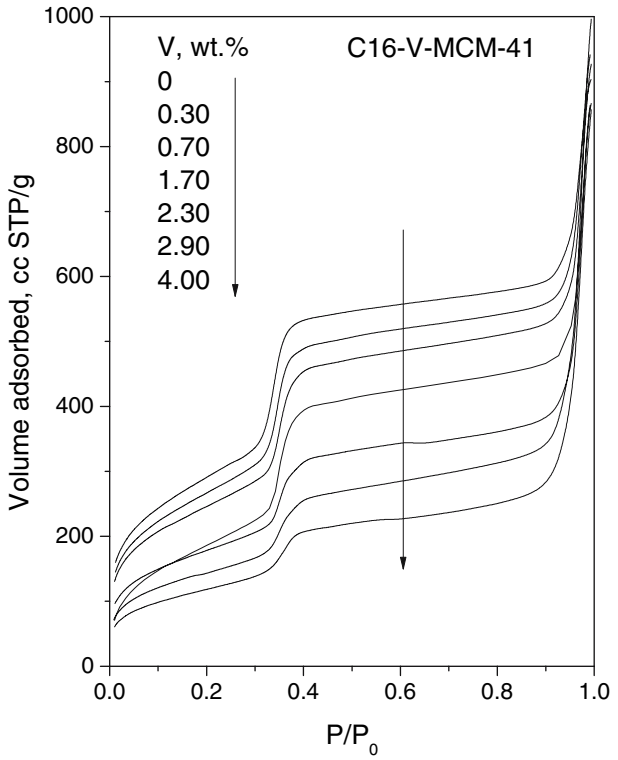

Fig. 1 Nitrogen adsorption of V-MCM-41 with different vanadium contents

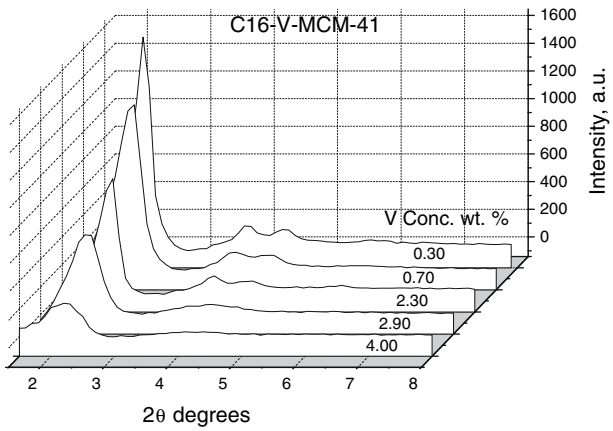

Fig. 2 X-ray diffractions of V-MCM-41 with different vanadium contents

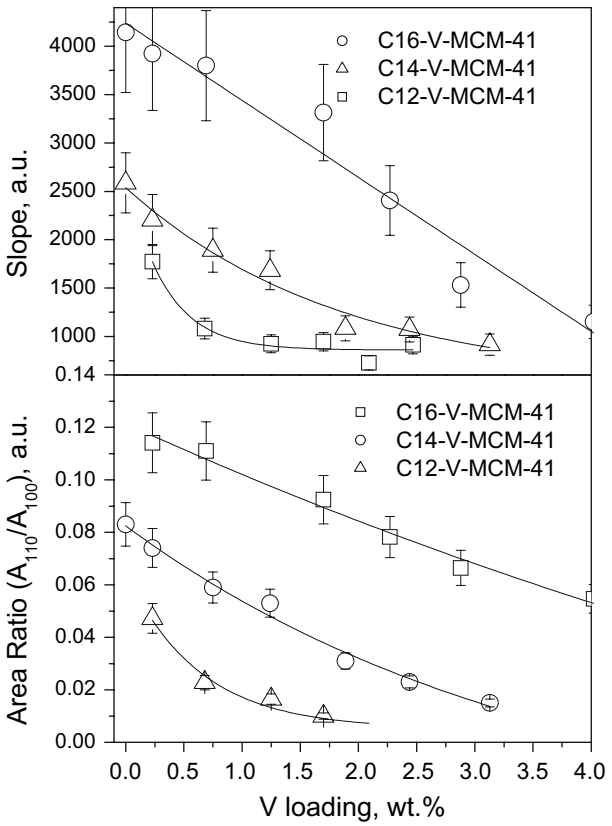

Fig. 3 Structure index of V-MCM-41 with different vanadium contents and different pore diameters

to 40%) was chosen to compensate the negative effect of vanadium incorporation for those C10 samples. Three samples were prepared with different TMA concentrations and vanadium contents (under pH 11.5). The results are shown in Fig. 4. High TMA group concentration (40%) improves the structure of C10-V-MCM-41 even though the initial vanadium content is high (0.6 wt.%), which can be found from more nitrogen volume adsorbed, higher surface area, and sharper pore size distribution.

3.2 Effect of Initial pH and the pH Evolution in the Synthesis Gel

X-ray diffraction was carried out to measure the hexagonal pore structures of V-MCM-41. All samples with different initial pH show highly ordered hexagonal pore structures indicated by four diffraction peaks as shown in Fig. 5. The intensities of the diffraction peaks decrease with the initial pH in the synthesis gel. The current synthesis procedure is to adjust the pH before the sample is put into the autoclave. However, it was found that the pH was not constant during the experiments. Fig. 6a shows that the pH drops from 11.5 to 11.2 after the synthesis for all the samples with different vanadium contents. In order to form the silica framework, it consumes OH^- to dissolve the neutral silica, which caused the decrease of pH. As for the different TMA group concentrations, the results are different depending on the initial conditions. Under low TMA concentration (<40%), the pH decreases after the synthesis; the pH will increase after the synthesis with higher initial TMA concentration (>40%), as shown in Fig. 6b. Klinowski and coworkers explained the chemistry and proposed reactions to understand the pH changing during the synthesis of MCM-41 materials [42]. Under low TMA concentration, the pH decreases according to the reaction:

$$\equiv \mathrm{Si{-}OH} + \mathrm{HO{-}SiO} \equiv \rightarrow \equiv \mathrm{SiOSi} \equiv + \mathrm{H_2O} \quad (1)$$

However, with more TMA groups, the pH abruptly increases during the nucleation period as a result of the formation of the zeolitic framework (composed of ≡ SiOSi ≡ units) via the condensation reaction:

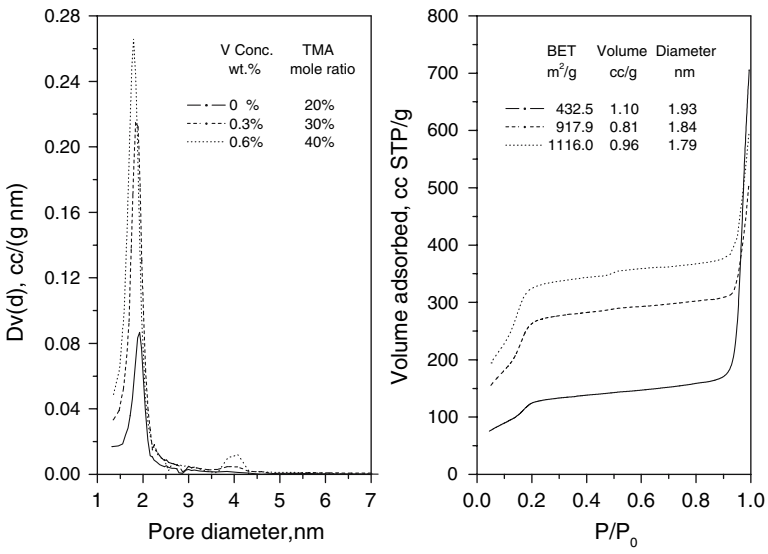

Fig. 4 Physical structures of V-MCM-41 with small pore diameter

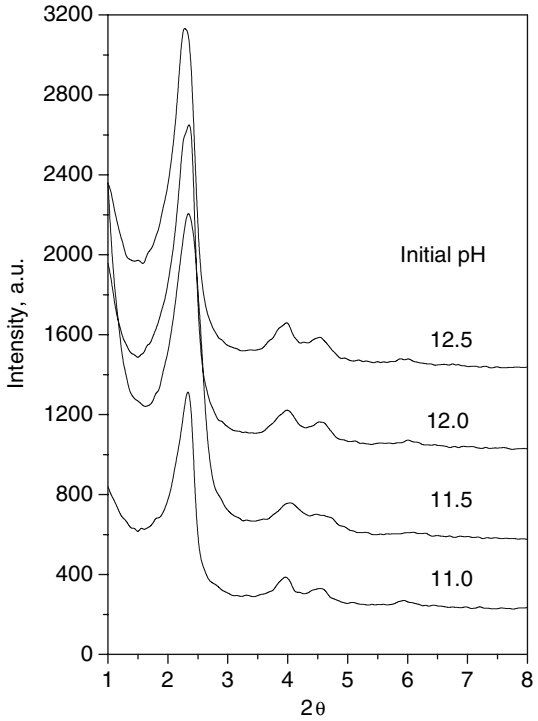

Fig. 5 pH effect on the physical structure of V-MCM-41

$$\equiv \mathrm{SiO^-} + \mathrm{HO{-}SiO} \equiv \rightarrow \equiv \mathrm{SiOSi} \equiv + \mathrm{OH^-} \quad (2)$$

3.3 Effect of the Template Surfactant

Mobil researchers have proposed that MCM-41 materials form via a liquid crystal templating mechanism [11, 12]. That is, a liquid crystalline phase forms initially and organizes silicate species in the continuous water region to create the inorganic walls of MCM-41. Alternatively, other researchers have proposed that the inorganic species could interact with the organic micelles to initiate the order of the organic and inorganic species [43]. Therefore, the nature of anionic species (e.g., halogen ions) is extremely important to control the formation of ordered templating micelle and highly ordered MCM-41 thereafter. Preparation of highly ordered MCM-41 with F^- anions under acidic conditions hydrothermal treatment by Huo et al. [44], and with hydrothermal restructuring by Sayari et al. have been reported [45].

In this work, surfactant containing either Br^- or Cl^- anions was used as a template to prepare MCM-41 sample respectively, the structures were measured by XRD and compared. It was difficult to prepare a good V-MCM-41 sample by using chloride ion containing surfactant, the mixture precipitates quickly and is hard to obtain homogeneous synthesis suspension. The intensities of XRD peaks of MCM-41 prepared using hexadecyltrimethylammonium chloride (CTACl) as the template are lower than that of hexadecyltrimethylammonium bromide (CTABr), which is consistent with the results reported by Cheng et al. [46]. The V-MCM-41 made by chlorine-containing surfactant has poor structural order compared to the samples made by bromine surfactant, which is indicated by the smaller (110) to (100) peak area ratios, as shown in Fig. 7. At room temperature, the solubility of CTABr in water is less that 10%, while that of CTACl exceeds 25%. ^{13}C NMR spectra of 7% aqueous solutions of CTACl and CTABr, in which both surfactants exist in the form of micelles shows that the solvation ability of CTACl is much higher than CTABr [46]. The spectral line widths from CTABr are greater that those from CTACl. The methyl group bonded to the nitrogen of the micelle head in CTABr is five times greater than that of CTACl because the quadrupolar Br^- anions are more difficult to solvate and interact more strongly with the cationic micelle head than the Cl^- anions, which will result in the MCM-41 with more uniform long-range order.

Figure 8 illustrates that different concentrations of templating surfactant strongly affect the quality of the

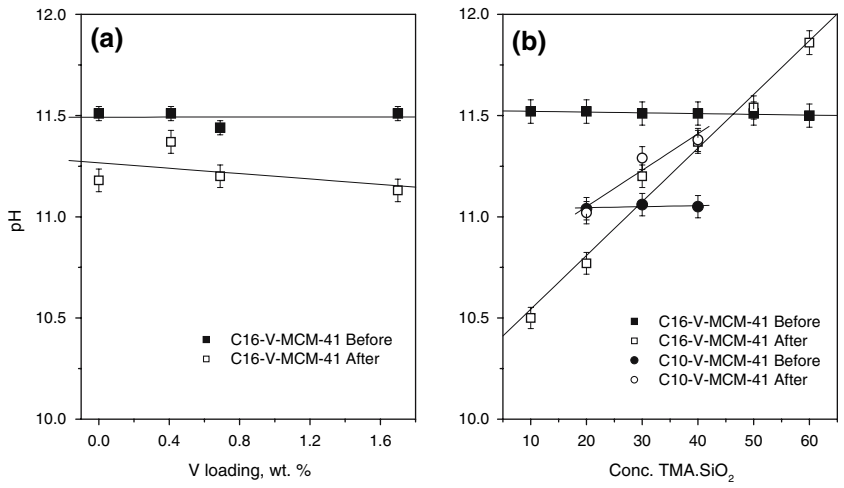

Fig. 6 pH evolutions under different synthesis conditions

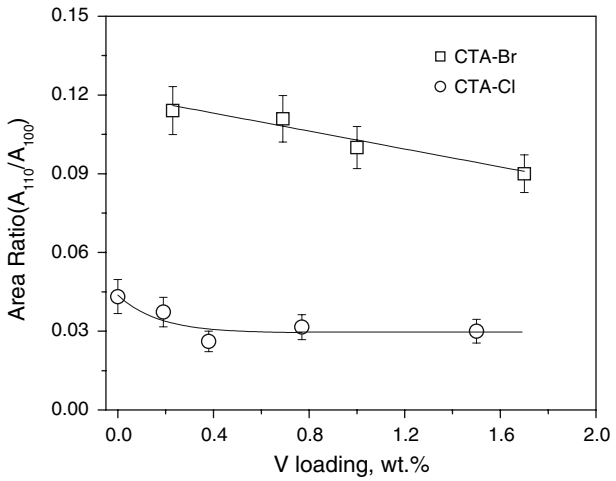

Fig. 7 Physical structures of V-MCM-41 prepared with different surfactants

product. The best quality MCM-41 in this study was prepared from a gel of composition of $1SiO_2$: 0.30 CTABr. Higher concentrations of surfactant have a clear detrimental effect because insufficient silica is available for the polymerization reaction.

3.4 Selective Oxidation of Cyclohexene

Liquid phase epoxidation was carried out in a three-neck flask under reflux. The reactor was heated in mineral oil bath. Certain amount of reactant, oxidant and substrate was loaded and well mixed by stirring. The mixture was brought to the reaction temperature before the catalyst was added. Sample solution was taken at selected reaction time, filtered and analyzed by a gas chromatograph (HP-6890) equipped with a HP-1 100 m × 0.5 mm × 0.25 μm capillary column. Different solvents (methanol, acetone, acetonitrile, and chloroform) and different oxidants (hydrogen peroxide and TBHP) were studied for the oxidation of cyclohexene. Products were identified by their retention time and mass spectra in a GC-MS system when necessary. The properties of the V-MCM-41 catalysts in this study are listed in Table 1.

Usually, large organic molecules reactions are hindered in small pore-size zeolites. Few active sites in the pores are accessible because of the pore size inhibition. The mesoporous catalysts, e.g., MCM-41, allow the synthesis of metal incorporated zeolite-like structures with larger pores, which makes the reaction of large organic molecules possible [25, 47]. Cyclohexene was oxidized very slowly to epoxide product in the presence of TS-1, such low reactivity has been attributed to the molecular dimension of cyclohexene, which can not enter the channels of TS-1 [48]. The pore diameters of the V-MCM-41 catalysts prepared in this study are from 1.8 to 2.9 nm, which is possible for most active sites to be accessible. The solvent can affect the catalytic activity in liquid phase reactions, different solvents result in a different distribution of the products. The solvents effect was studied first by reacting

Table 1

	Slope of capillary condensation a.u.	Pore diameter nm	Surface area m^2/g	*V* conc. wt.%
C10-V-MCM-41	736	1.80	505	0.26
C12-V-MCM-41	2231	2.27	736	0.52
C14-V-MCM-41	4411	2.60	749	0.67
C16-V-MCM-41	7144	2.91	790	0.66

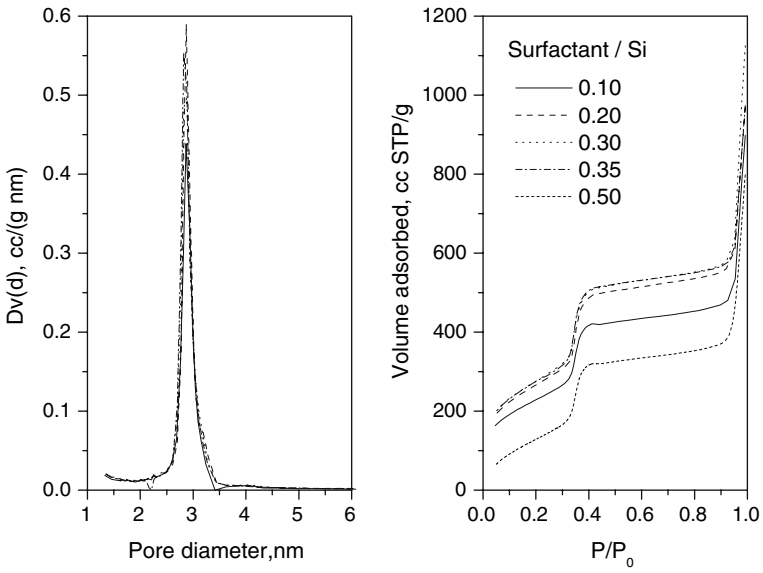

Fig. 8 Surfactant content effect on the V-MCM-41 structures

cyclohexene with hydrogen peroxide or *t*-butyl hydroperoxide in methanol, acetone, acetonitrile and chloroform. There were no products formed in the absence of the catalyst, even at high temperature. After the catalyst was introduced, products were formed immediately. According to the literature, a straightforward formation of cyclohexene oxide should be expected. However, when the solvent was methanol, acetone, and acetonitrile, epoxide cannot be quantitatively identified by gas chromatograph because it reacted with the solvent and precipitated from the solvent, which can not be separated from the catalyst. There was no such analysis problem for the solvent of chloroform. When the oxidant was switched from H_2O_2 to *t*-butyl hydroperoxide (TBHP), there was a significant increase in the reactivity. Thus, the reactions were mostly studied in the chloroform solvent using *t*-butyl hydroperoxide as the oxidant. For the oxidation of cyclohexene, the temperature has a positive effect. Increasing temperature will increase the reaction rate, and such temperature effect is reproducible, shown in Fig. 9. Figures 10 and 11 show the results of cyclohexene conversion and the production of cyclohexene oxide, there is a clear pore wall curvature effect, especially for the first 7 h. One important advantage of MCM-41 materials is that their pore size can be easily controlled by using surfactant with different alkyl chain length. The pore size increases monotonically from C10–C16 and corresponds with the conversion of cyclohexene and cyclohexene oxide production for the first several hours of the reaction. The reaction was proposed to be a radical mechanism. According to Mimoun et al., the vanadium peroxo radical is believed to be the active species for the transfer of oxygen to reactants in the liquid phase reaction [49]. The reduction of V^{5+} to V^{4+} is required for the formation of the peroxo radicals, which is favored by highly dispersed V in the molecular sieves. For the first several hours, *t*-butyl hydroperoxide enters the channels of V-MCM-41, reacting with the vanadium to form vanadium peroxo radicals. This step is dependent on the pore size of the catalyst; within a certain time, the amount of *t*-butyl hydroperoxide enters the pores is affected by the pore

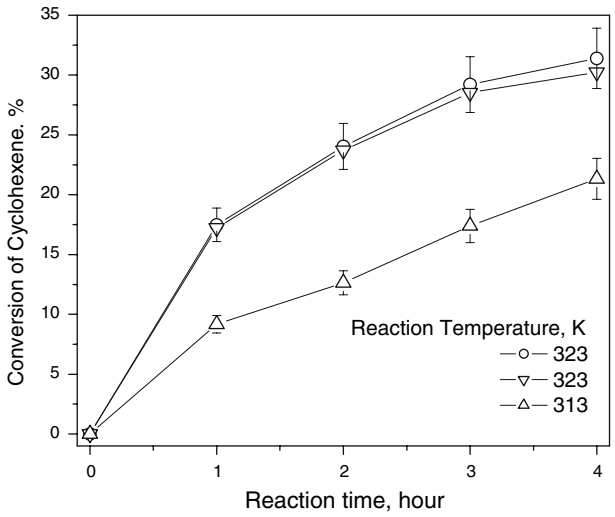

Fig. 9 Temperature effect on the reactivities

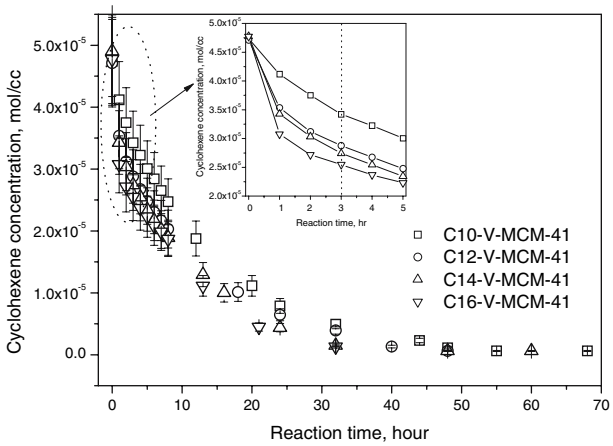

Fig. 10 Pore wall curvature effect on the cyclohexene conversions

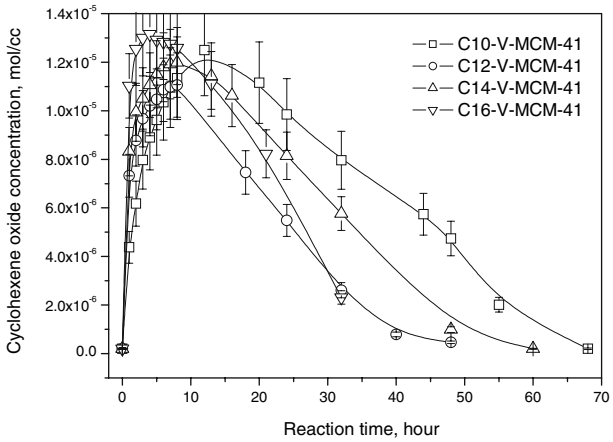

Fig. 11 Pore wall curvature effect on the production of cyclohexene oxides

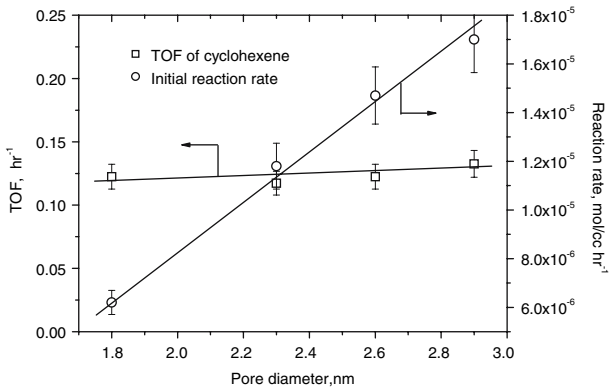

Fig. 12 Comparison between initial reactivity and turnover numbers of cyclohexene oxidation

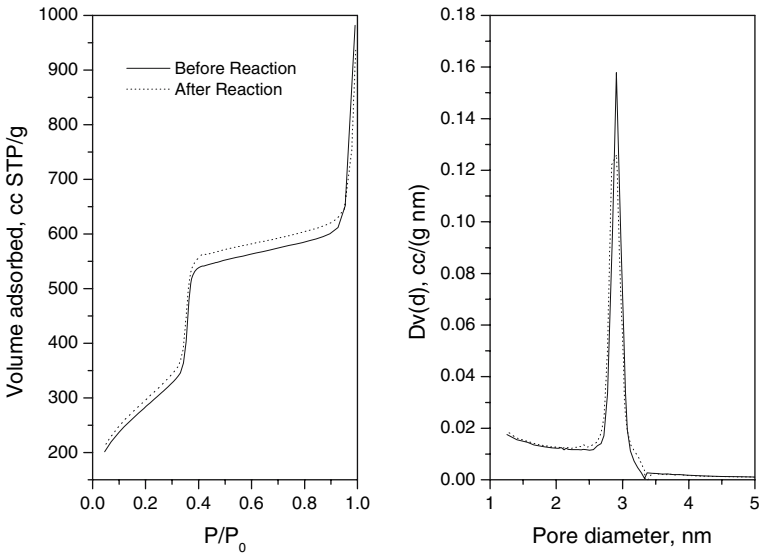

Fig. 13 Physical structures of V-MCM-41 before and after the reactions

channels. Larger pores allow more *t*-butyl hydroperoxide to enter. Once the vanadium peroxo radical formation, the conversion does not depend on the pore size of V-MCM41 due to the strong pore diffusion limitation of liquid reactant and products, which has been summarized in Fig. 12. The initial reaction rate is a liner function of pore size, and the total turnover frequency over longer time is constant respect to V-MCM-41 catalysts with different pore diameters. If the reaction runs for a longer time, cyclohexene oxide will continue to react with the solvent to form 2-chlorocyclohexanol. The time required to reach the maximum production of cyclohexene oxide has the same porosity effect as the conversion of cyclohexene. The maximum conversion of cyclohexene oxide occurs at 4 h for C16-V-MCM-41. With the decrease of pore size, the maximum conversion time increases, this can also be explained by the slower reaction rate with smaller pore size catalyst applied. The catalyst after 72-h reaction shows the identical isotherms as before the reaction, as shown in Fig. 13, it means that the ordered pore structures has been remained after reaction. Negligible leaching vanadium component was found in the reaction solution (tested by ICP analysis) because of the strong chemical bond between vanadium and the MCM-41 supports.

4 Conclusion

V-MCM-41 samples with similar surface area and vanadium content but different pore diameters have been prepared, the effect of vanadium loading, surfactant chain length and type, pH has been discussed. V-MCM-41 shows high reactivity in the selective oxidation of cyclohexene. The pore wall radius of curvature effect in the liquid phase reaction was investigated. The initial reaction rates were observed to strongly correlate with the pore diameters, the larger the pore size, the higher the initial reaction rate due to higher accessibility of vanadium components in the pore walls. The overall turnover numbers for a long period was constant respect to the different pore sizes which is probably due to the strong pore diffusion limitation in the liquid phase reaction. The physical structure of V-MCM-41 samples has been well maintained due to their high stability. Negligible vanadium was lost because of the leaching.

Acknowledgment We are grateful to the Start-up Grant, Nanyang Technological University, Singapore, for financial support. We also thank to AcRF grant RG45/06 and AcRF grant RG118/06 for financial support.

References

1. Deo G, Wachs IE (1994) J Catal 146:323
2. Parvulescu V, Anastasescu C, Constantin C, Su BL (2002) In: Impact of zeolites and other porous materials on the new technologies at the beginning of the new millennium, Pts a and B, vol 142. pp 1213
3. Parvulescu V, Dascalescu C, Su BL (2003) In: Nanotechnology in mesostructured materials, vol 146. pp 629
4. Parvulescu V, Su BL (2001) Catal Today 69:315
5. Solsona B, Blasco T, Nieto JML, Pena ML, Rey F, Vidal-Moya A (2001) J Catal 203:443
6. Ziolek M (2004) Catal Today 90:145
7. Corma A, Martinez A (1995) Adv Mater 7:137
8. Davis ME, Lobo RF (1992) Chem Mater 4:756
9. Feijen EJP, Martens JA, Jacobs PA (1994) In: Zeolites and related microporous materials: state of the art, vol 84. pp 3
10. Flanigen EM (1976) In: JA Rabo (ed) ACS monograph series 1971. American Chemical Society, Washington DC
11. Beck JS, Vartuli JC, Roth WJ, Leonowicz ME, Kresge CT, Schmitt KD, Chu CTW, Olson DH, Sheppard EW, McCullen SB, Higgins JB, Schlenker JL (1992) J Am Chem Soc 114:10834
12. Kresge CT, Leonowicz ME, Roth WJ, Vartuli JC, Beck JS (1992) Nature 359:710

13. Ortlam A, Rathousky J, SchulzEkloff G, Zukal A (1996) Microporous Mater 6:171
14. Kruk M, Jaroniec M, Sayari A (1997) Langmuir 13:6267
15. Edler KJ, Reynolds PA, White JW, Cookson D (1997) J Chem Soc-Faraday Transac 93:199
16. Ravikovitch PI, Wei D, Chueh WT, Haller GL, Neimark AV (1997) J Phys Chem B 101:3671
17. Lukens WW, Schmidt-Winkel P, Zhao DY, Feng JL, Stucky GD (1999) Langmuir 15:5403
18. Lim MH, Stein A (1999) Chem Mat 11:3285
19. Kalipcilar H, Culfaz A (2000) Cryst Res Technol 35:933
20. Lim S, Ciuparu D, Pak C, Dobek F, Chen Y, Harding D, Pfefferle L, Haller G (2003) J Phys Chem B 107:11048
21. Yang YH, Lim S, Wang C, Harding D, Haller G (2004) Microporous Mesoporous Mater 67:245
22. Amama PB, Lim S, Ciuparu D, Yang YH, Pfefferle L, Haller GL (2005) J Phys Chem B 109:2645
23. Tanev PT, Chibwe M, Pinnavaia TJ (1994) Nature 368:321
24. Zhao DY, Goldfarb, D (1995) J Chem Soc-Chem Commun 875
25. Reddy KM, Moudrakovski I, Sayari A (1994) J Chem Soc-Chem Commun 1059
26. Sayari A, Moudrakovski I, Danumah C, Ratcliffe CI, Ripmeester JA, Preston KF (1995) J Phys Chem 99:16373
27. Yuan ZY, Liu SQ, Chen TH, Wang JZ, Li HX (1995) J Chem Soc-Chem Commun 973
28. Berndt H, Martin A, Bruckner A, Schreier E, Muller D, Kosslick H, Wolf GU, Lucke B (2000) J Catal 191:384
29. Centi G, Perathoner S, Trifiro F, Aboukais A, Aissi CF, Guelton M (1992) J Phys Chem 96:2617
30. Dzwigaj S, Krafft JM, Che M, Lim S, Haller GL (2003) J Phys Chem B 107:3856
31. Lim S, Haller GL (2002) J Phys Chem B 106:8437
32. Lim SY, Haller GL (1999) Appl Catal A-Gen 188:277
33. Reddy EP, Davydov L, Smirniotis PG (2002) J Phys Chem B 106:3394
34. Wei D, Chueh WT, Haller GL (1999) Catal Today 51:501
35. Wei D, Wang H, Feng XB, Chueh WT, Ravikovitch P, Lyubovsky M, Li C, Takeguchi T, Haller GL (1999) J Phys Chem B 103:2113
36. Yang YH, Du GA, Lim SY, Haller GL (2005) J Catal 234:318
37. Dai PE, Lunsford JH (1980) J Catal 64:184
38. Guo J, Jiao QZ, Shen JP, Jiang DZ, Yang GH, Min EZ (1996) Catal Lett 40:43
39. Corma A, Navarro MT, Pariente JP (1994) J Chem Soc-Chem Commun 147
40. Barrett EP, Joyner LG, Halenda PP (1951) J Am Chem Soc 73:373
41. Kruk M, Jaroniec M, Sayari A (1997) J Phys Chem B 101:583
42. Cheng CF, Park DH, Klinowski J (1997) J Chem Soc-Faraday Transac 93:193
43. Huo QS, Leon R, Petroff PM, Stucky GD (1995) Science 268:1324
44. Huo QS, Margolese DI, Ciesla U, Feng PY, Gier TE, Sieger P, Leon R, Petroff PM, Schuth F, Stucky GD (1994) Nature 368:317
45. Sayari A, Liu P, Kruk M, Jaroniec M (1997) Chem Mater 9:2499
46. Cheng CF, Park DH, Klinowski J (1997) J Chem Soc-Faraday Transac 93:193
47. Blasco T, Corma A, Navarro MT, Pariente JP (1995) J Catal 156:65
48. Li C, Xiong G, Xin Q, Liu JK, Ying PL, Feng ZC, Li J, Yang WB, Wang YZ, Wang GR, Liu XY, Lin M, Wang XQ, Min EZ (1999) Angewandte Chemie—International Edition 38:2220
49. Mimoun H, Saussine L, Daire E, Postel M, Fischer J, Weiss R (1983) J Am Chem Soc 105:3101